



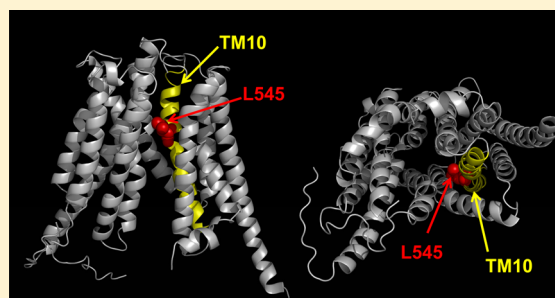
## Cysteine Scanning Mutagenesis of Transmembrane Domain 10 in Organic Anion Transporting Polypeptide 1B1

Shuichi Ohnishi,<sup>†</sup> Amanda Hays,<sup>†</sup> and Bruno Hagenbuch<sup>\*,†,‡</sup>

<sup>†</sup>Department of Pharmacology, Toxicology and Therapeutics, The University of Kansas Medical Center, Kansas City, Kansas 66160, United States

<sup>‡</sup>University of Kansas Cancer Center, Kansas City, Kansas 66160, United States

**ABSTRACT:** Organic anion transporting polypeptide (OATP) 1B1 is an important drug transporter expressed in human hepatocytes. Previous studies have indicated that transmembrane (TM) domain 2, 6, 8, 9, and in particular 10 might be part of the substrate binding site/translocation pathway. To explore which amino acids in TM10 are important for substrate transport, we mutated 34 amino acids individually to cysteines, expressed them in HEK293 cells, and determined their surface expression. Transport activity of the two model substrates estrone-3-sulfate and estradiol-17 $\beta$ -glucuronide as well as of the drug substrate valsartan for selected mutants was measured. Except for F534C and F537C, all mutants were expressed at the plasma membrane of HEK293 cells. Mutants Q541C and A549C did not transport estradiol-17 $\beta$ -glucuronide and showed negligible estrone-3-sulfate transport. However, A549C showed normal valsartan transport. Pretreatment with the anionic and cell impermeable sodium (2-sulfonatoethyl)methanethiosulfonate (MTSES) affected the transport of each substrate differently. Pretreatment of L545C abolished estrone-3-sulfate uptake almost completely, while it stimulated estradiol-17 $\beta$ -glucuronide uptake. Further analyses revealed that mutant L545C in the absence of MTSES showed biphasic kinetics for estrone-3-sulfate that was converted to monophasic kinetics with a decreased apparent affinity, explaining the previously seen inhibition. In contrast, the apparent affinity for estradiol-17 $\beta$ -glucuronide was not changed by MTSES treatment, but the  $V_{\max}$  value was increased about 4-fold, explaining the previously seen stimulation. Maleimide labeling of L545C was affected by preincubation with estrone-3-sulfate but not with estradiol-17 $\beta$ -glucuronide. These results strongly suggest that L545C is part of the estrone-3-sulfate binding site/translocation pathway but is not directly involved in binding/translocation of estradiol-17 $\beta$ -glucuronide.



Organic anion transporting polypeptides (OATPs, gene symbol *SLCO*) are solute carrier superfamily members that mediate the sodium-independent transport of a wide range of amphipathic organic compounds including bile acids, steroid conjugates, thyroid hormones, anionic peptides, numerous drugs, and other xenobiotic substances.<sup>1,2</sup> Among the 11 human OATPs, OATP1B1 is one of two liver-specific OATPs. It is a glycoprotein of 691 amino acids with an apparent molecular mass of approximately 84 kDa and 12 putative transmembrane domains.<sup>3</sup> Under normal physiological conditions, this transporter seems to be exclusively expressed at the basolateral membrane of human hepatocytes<sup>4</sup> and plays a pivotal role in the uptake of numerous drugs including statins and sartans from the portal and systemic blood into hepatocytes.<sup>2,5</sup> Several studies have shown the possible involvement of OATP1B1 in drug–drug interactions. For example, in organ transplant patients, the OATP1B1 inhibitor cyclosporine A increased the mean AUC of fluvastatin,<sup>6</sup> pravastatin,<sup>7</sup> and rosuvastatin,<sup>8</sup> which are all substrates of OATP1B1. Pharmacogenomic correlation studies revealed that the *SLCO1B1* c.521 T > C SNP was associated with myopathy in 85 patients who were taking 80 mg of simvastatin daily.<sup>9</sup> Thus, OATP1B1 can be the cause of interindividual variance in drug pharmacokinetics, and it could be used as an effective

target for rational drug design to improve lack of drug efficacy or prevent adverse side effects.

Computer-based *in silico* approaches have become powerful tools to virtually predict transporter–ligand interactions.<sup>10,11</sup> They can be performed from two different perspectives: either ligand-based or transporter-based. With respect to the ligand-based method for substrates of OATP1B1, a pharmacophore model was generated with published  $K_m$  values, and it demonstrated that the key molecular features for substrate transporter interactions appeared to be two hydrogen bond acceptors at either end of a large hydrophobic area.<sup>12</sup> Similar structure requirements for OATP1B1 substrates were also derived from comparative molecular field analysis (CoMFA) on the basis of competitive inhibitors of estradiol-17 $\beta$ -glucuronide.<sup>13</sup> In contrast, transporter protein-based methods for OATP1B1 are currently limited because there is no high resolution crystal structure available. As an alternative, homology models for OATP1B1, OATP1B3, and OATP2B1 have been generated based on the known structure of bacterial

**Received:** February 7, 2014

**Revised:** March 26, 2014

**Published:** March 27, 2014



major facilitator superfamily transporters.<sup>14–17</sup> On the basis of these models, several groups using chimeric proteins and site-directed mutagenesis have identified transmembrane (TM) domains 2, 6, 8, 9, and 10 to be important for proper function of OATP1B1.<sup>17–20</sup> Furthermore, positive amino acid residues R57, K361, and R580 seem to be part of the substrate binding and/or translocation pathways in OATP1B1.<sup>21</sup> In addition, a recent report showed that amino acids at positions 45, 545, and 615 in OATP1B1 are crucial for substrate recognition. When these amino acids were replaced by the corresponding amino acids found in OATP1B3, OATP1B1 was able to transport the OATP1B3-selective substrate cholecystokinin 8.<sup>22</sup> In the present study, we focused on TM10 of OATP1B1 and performed cysteine scanning mutagenesis to determine accessibility and potential involvement of individual amino acid positions in the substrate binding site/translocation pathway. The results of this study will help to better understand the multispecificity of OATP1B1 and eventually help in predicting and preventing adverse drug–drug interactions.

## EXPERIMENTAL PROCEDURES

**Materials.** Radiolabeled [<sup>3</sup>H]estrone-3-sulfate (57.3 Ci/mmol) and [<sup>3</sup>H]estradiol-17 $\beta$ -glucuronide (46.9 Ci/mmol) were purchased from Perkin-Elmer (Boston, MA). Unlabeled estrone-3-sulfate and estradiol-17 $\beta$ -glucuronide were purchased from Sigma Aldrich (St. Louis, MO). Unlabeled valsartan, MTSES, and [2-(trimethylammonium)ethyl]-methanethiosulfonate bromide (MTSET) were purchased from Toronto Research Chemicals, Inc. (North York, Ontario, Canada). Sulfo-NHS-SS-biotin and maleimide-PEG<sub>2</sub>-biotin were purchased from Pierce Biotechnology (Rockford, IL). The polyclonal anti-His antibody was purchased from Covance (Princeton, IL), whereas the monoclonal antibody to detect Na<sup>+</sup>/K<sup>+</sup> ATPase  $\alpha$  subunit was purchased from Abcam (Boston, MA).

**Site-Directed Mutagenesis.** The previously described human OATP1B1\*1b with a six His-tag at the C-terminal end in the pcDNA5/FRT vector was used for all experiments.<sup>20</sup> Site-directed mutations were performed with the Quick Change site-directed mutagenesis kit (Stratagene, La Jolla, CA) using primers containing the codon for cysteine (either TGT or TGC) flanked by 18 perfectly matching nucleotides on both sides. All mutants were verified by DNA sequencing.

**Cell Culture and Transfection.** Human embryonic kidney (HEK293) cells were grown as previously described.<sup>15</sup> HEK293 cells were plated at 250 000 cells/well on 24-well plates for transport assays or at 1 250 000 cells/well on six-well plates for surface biotinylation. Twenty-four hours later, OATP1B1 and the respective cysteine mutants were transiently transfected using FuGENE HD Transfection Reagent following the manufacturer's protocol (Roche, Mannheim, Germany), and 48 h later the transfected cells were used for the assays.

**Transport Assay.** Uptake was performed according to a previously published method.<sup>21</sup> Briefly, HEK293 cells were carefully washed with prewarmed uptake buffer (142 mM NaCl, 5 mM KCl, 1 mM KH<sub>2</sub>PO<sub>4</sub>, 1.2 mM MgSO<sub>4</sub>, 1.5 mM CaCl<sub>2</sub>, 5 mM glucose, and 12.5 mM HEPES, pH 7.4) and then incubated with 200  $\mu$ L of uptake buffer containing substrate for the indicated time periods at 37 °C. Uptake was stopped by removing the substrate solution and washing the cells with ice-cold uptake buffer. To determine uptake of [<sup>3</sup>H]estrone-3-sulfate and [<sup>3</sup>H]estradiol-17 $\beta$ -glucuronide, the cells were then solubilized with 300  $\mu$ L of 1% Triton X-100 per well and 200

$\mu$ L were used for liquid scintillation counting. From the remaining lysate, protein concentration was determined for each well using the BCA protein assay kit. For the uptake of valsartan, the cells in each well were treated with 135  $\mu$ L of 7.5 mM ammonium formate (pH 5.0)/acetonitrile/methanol = 2:1:1 by volume containing 15  $\mu$ L of losartan (100 ng/mL, analytical internal standard) for 20 min at room temperature with constant agitation. After centrifugation, the supernatants were subjected to LC/MS/MS analysis. Cells transfected with the empty vector served as background control in all experiments. Kinetic experiments were performed under initial linear rate conditions. To calculate transporter-specific uptake, the values obtained with empty vector transfected cells were subtracted from the values obtained with cells transfected with OATP1B1 or its mutants, and the resulting uptake values were normalized for surface expression levels of the constructs. When the effects of MTSES or MTSET were investigated, cells were pretreated with uptake buffer in the absence or presence of 10 mM MTSES or 10 mM MTSET for 10 min at 37 °C.

**Cell Surface Biotinylation and Western Blotting.** Cell surface biotinylation was performed essentially following a published procedure.<sup>23</sup> Forty-eight hours after transfection, HEK293 cells were washed with ice-cold phosphate-buffered saline (PBS, pH 7.4) and treated with sulfo-NHS-SS-biotin (1 mg/mL in PBS, pH 7.4) for 1 h at 4 °C. Cells were lysed and the biotinylated proteins were captured using NeutrAvidin beads (Pierce Biotechnology), and after centrifugation the biotinylated proteins were recovered by incubating the beads with 2 $\times$  Laemmli buffer containing 50 mM DTT for 30 min at room temperature. Samples were separated using SDS-polyacrylamide gel electrophoresis and transferred to a nitrocellulose membrane. OATP1B1 and its cysteine mutants were detected using a polyclonal anti-His antibody (1:2500 dilution), followed by horseradish peroxidase-conjugated goat anti-rabbit IgG (1:10000 dilution). Na<sup>+</sup>/K<sup>+</sup>-ATPase was used as loading control for normalization and was detected with a mouse anti-Na<sup>+</sup>/K<sup>+</sup>-ATPase  $\alpha$  subunit antibody (1:5000 dilution). ECL plus (Amersham Biosciences, Piscataway, NJ) was used for detection. Protein band intensities were quantified with the Quantity One analysis software (Bio-Rad Laboratories, Hercules, CA).

**Maleimide Biotinylation.** Forty-eight hours after transfection, HEK293 cells were washed with prewarmed uptake buffer (37 °C, pH 7.4) and then incubated with either uptake buffer alone or uptake buffer containing 10 mM MTSES or 10 mM MTSES and 1 mM estrone-3-sulfate or 10 mM MTSES and 0.75 mM estradiol-17 $\beta$ -glucuronide for 10 min at 37 °C to label the accessible cysteines. Then, cells were washed with ice-cold phosphate-buffered saline (PBS, pH 7.0) and treated with maleimide-PEG<sub>2</sub>-biotin (0.5 mg/mL in PBS, pH 7.0) for 1 h at 4 °C. The biotinylated protein was captured using NeutrAvidin beads and then recovered from the beads by boiling with 2 $\times$  Laemmli buffer containing 50 mM DTT for 5 min. Samples were separated using SDS-polyacrylamide gel electrophoresis and after transfer to nitrocellulose membranes analyzed as described above.

**Determination of Valsartan by LC/MS/MS Analysis.** Standard curves were prepared in the respective cell lysate matrix and used for each analysis. Losartan was used as analytical internal standard at a concentration of 10 ng/mL. The LC/MS/MS system consisted of a Shimadzu LC-20AD (Shimadzu Corporation, Kyoto, Japan) and a Waters Quattro Premiere mass spectrometer (Waters Corporation, Milford,

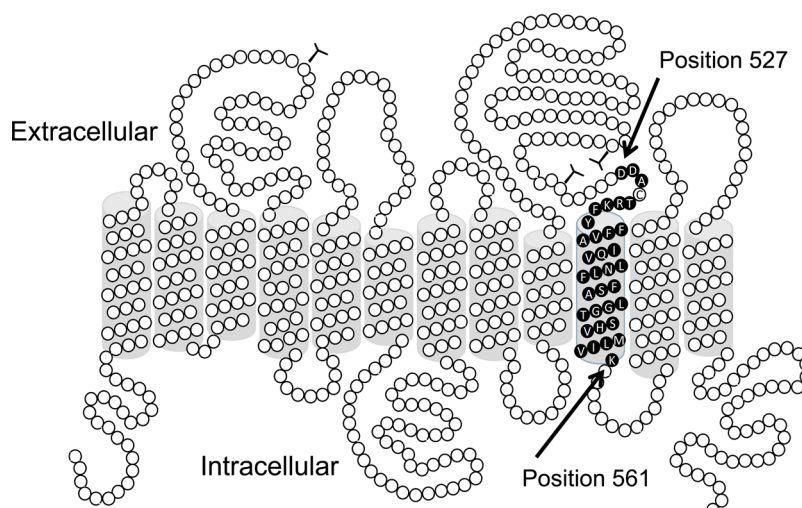


**Figure 1.** Predicted membrane topology of OATP1B1. The mutated amino acids in transmembrane domain 10 (between amino acid positions 527 and 561) are indicated with black circles.

MA). The desolvation gas (nitrogen) flow rate was 650 L/h, the cone gas (nitrogen) flow rate was 60 L/h, the source temperature was 120 °C, and the desolvation temperature was 350 °C.

The mass spectrometer was operated in multiple reaction monitoring mode using positive ion electrospray (ESI). The valsartan product ion was formed using a capillary energy of 2.5 kV and a cone energy of 30 V. Product ion formed at the collision energy of 22 eV ( $m/z$  436.39  $\rightarrow$  207.20) was monitored. The mobile phase used for high-performance liquid chromatography was 7.5 mM ammonium formate (pH 5.0)/acetonitrile/methanol = 2:1:1 by volume, and the flow rate was 0.5 mL/min. Chromatographic separation was achieved on a Luna C-18 column (5  $\mu$ m, 50  $\times$  2 mm) fitted with a C18 guard column (Phenomenex, Torrance, CA).

**Data Analysis.** Statistical significance was calculated using two-tailed unpaired Student's  $t$  test, and  $P < 0.05$  was considered significant (SigmaPlot 12.0, Systat Software, Inc., Point Richmond, CA). To obtain apparent  $K_m$  and  $V_{max}$  values, nonlinear regression analysis was performed, and the experimental data were plotted using Eadie–Hofstee plots.

## RESULTS

To determine to what extent cysteine replacement of the amino acids in TM10 (Figure 1) would affect the functional activity of OATP1B1, wild-type OATP1B1 and each of the cysteine mutants were transiently expressed in HEK293 cells. Figure 2A demonstrates that most mutants were able to mediate uptake of both OATP-model substrates estrone-3-sulfate and estradiol-17 $\beta$ -glucuronide. Transport of each substrate was negligible in each of the mutants F534C, F537C, Q541C, and A549C. Surface expression analysis (Figure 2B) revealed that F534C and F537C were not expressed at the surface. Western blot analysis of whole cell lysates demonstrated that mutants F534C and F537C were synthesized as unglycosylated proteins of 60 kDa instead of 84 kDa (data not shown) suggesting that these two mutations affect protein stability, folding, and/or trafficking, and they were omitted from further analysis. In contrast, although Q541C and A549C did only show minimal substrate uptake (less than 20% of estrone-3-sulfate transport and less than 2% of estradiol-17 $\beta$ -glucuronide transport of wild-type OATP1B1), their surface expression levels were

comparable to wild-type OATP1B1. However, because of their overall low transport function, these two mutants were also omitted from further analysis. Because surface expression of the different mutants after correction with the loading control  $\text{Na}^+/\text{K}^+$  ATPase was variable, all further functional results were corrected for their surface expression levels. Compared to wild-type OATP1B1 cysteine mutants of amino acid residues in the second half of TM10 (Figure 1) showed overall reduced substrate transport (Figure 2C). Mutating G551 to a cysteine residue resulted in about a 2-fold increase in estrone-3-sulfate uptake compared to wild-type OATP1B1, while estradiol-17 $\beta$ -glucuronide uptake was not affected.

After it was established that most mutants were functional, the effect of the negatively charged and membrane impermeable MTSES on wild-type OATP1B1 and its different cysteine mutants was examined. Figure 3A summarizes the results obtained for estrone-3-sulfate uptake and shows that wild-type OATP1B1 and most of the tested mutants were not affected, at least for this substrate, by preincubation with MTSES. Estrone-3-sulfate uptake by R532C, V542C, L545C, G551C, T553C, and V556C was significantly inhibited by pretreatment with MTSES. Interestingly, MTSES pretreatment also resulted in stimulation of estrone-3-sulfate uptake for S548C and G552C. In the case of estradiol-17 $\beta$ -glucuronide uptake (Figure 3B), MTSES pretreatment resulted in reduced uptake for G552C, H555C, and V556C, while uptake by N544C and L545C was stimulated by 3- and 6-fold, respectively.

Because MTSES affected L545C most strongly, resulting in inhibition of estrone-3-sulfate but stimulation of estradiol-17 $\beta$ -glucuronide uptake, kinetic analyses of both substrates were performed to determine to what extent apparent affinity and maximal transport rates were affected by MTSES pretreatment. The Eadie–Hofstee plot in Figure 4A clearly shows that like wild-type OATP1B1<sup>20,24,25</sup> mutant L545C exhibits biphasic transport kinetics of estrone-3-sulfate with a high affinity low capacity ( $K_{m1} = 0.9 \mu\text{M}$ ;  $V_{max1} = 95.9 \text{ pmol/normalized mg/min}$ ) and a low affinity high capacity ( $K_{m2} = 15.6 \mu\text{M}$ ;  $V_{max2} = 298 \text{ pmol/normalized mg/min}$ ) component (Table 1). However, after pretreatment with MTSES only a single  $K_m$  value of 89.7  $\mu\text{M}$  and a  $V_{max}$  value of 1018 pmol/normalized mg/min could be calculated (Table 1) indicating that for estrone-3-sulfate transport the presence of MTSES on L545



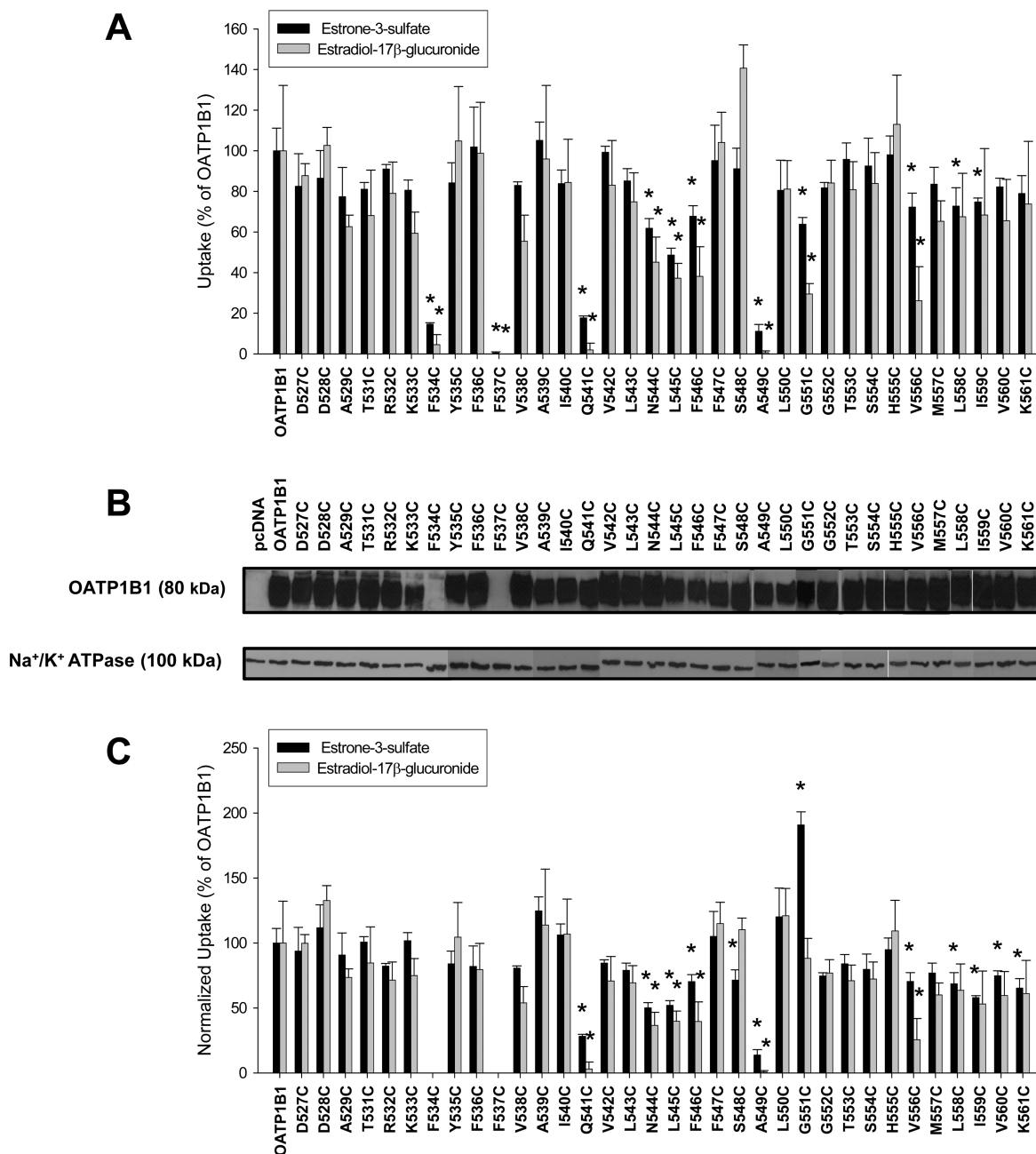


**Figure 2.** Substrate transport and surface expression of OATP1B1 and the TM10 cysteine mutants. (A) Uptake of 0.1  $\mu$ M [ $^3$ H]estrone-3-sulfate (black bars) or 1  $\mu$ M [ $^3$ H]estradiol-17 $\beta$ -glucuronide (gray bars) was measured with HEK293 cells transfected with empty vector, OATP1B1, or 34 cysteine mutants at 37  $^{\circ}$ C for 30 s (estrone-3-sulfate) or 2 min (estradiol-17 $\beta$ -glucuronide), respectively. After the values obtained with empty vector transfected cells were subtracted, results were calculated as a percentage of uptake activity for OATP1B1. Each bar is the mean  $\pm$  SD of three individual experiments. An asterisk (\*) indicates values significantly different from that of OATP1B1 ( $p < 0.05$ ). The amino acid on the left side (D527) is located close to the predicted extracellular side of TM10, while the one on the right side (K561) is located at the predicted cytoplasmic side of TM10. (B) Biotinylated membrane proteins were subjected to Western blot analysis with an anti-His antibody detecting the C-terminal end of OATP1B1 and the mutant proteins. The plasma membrane marker Na<sup>+</sup>/K<sup>+</sup> ATPase  $\alpha$  subunit was used as protein loading control. (C) Uptake values shown in (A) were corrected for protein expression and are given as normalized uptake. Asterisks (\*) indicate values significantly different from that of OATP1B1 ( $p < 0.05$ ).

affects both apparent binding affinity as well as substrate translocation. In contrast, the Eadie–Hofstee plot for estradiol-17 $\beta$ -glucuronide uptake (Figure 4B) shows only a single phase and demonstrates that in the presence of MTSES the apparent affinity is not changed (Table 1), but the  $V_{\max}$  value is increased about 4-fold (Table 1).

To more directly test whether L545 is involved in substrate binding, we tested whether MTSES-labeling of L545C could be

protected by the presence of substrate using maleimide biotinylation. In these experiments, cells transfected with empty vector, wild-type OATP1B1, or mutant L545C were treated with maleimide-PEG<sub>2</sub>-biotin for 1 h at 4  $^{\circ}$ C after having been preincubated with uptake buffer (Figure 5; Control) for 10 min at 37  $^{\circ}$ C. Cell lysates were then treated with NeutrAvidin beads, and after a centrifugation step bound proteins were subjected to Western blot analysis using an anti-

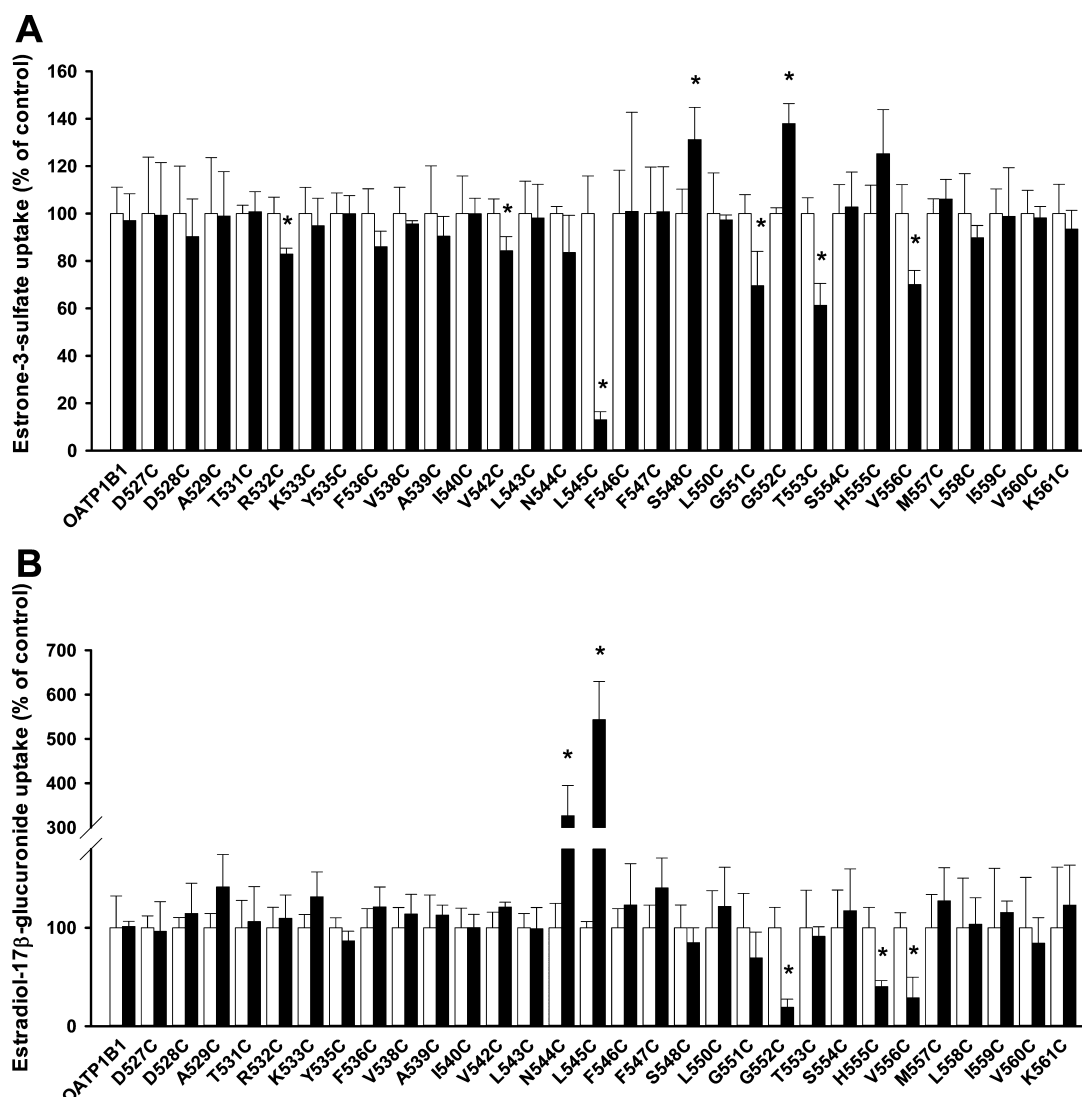


**Figure 3.** Effect of MTSES on estrone-3-sulfate and estradiol-17β-glucuronide uptake by OATP1B1 and its TM10 cysteine mutants. HEK293 cells transfected with empty vector, OATP1B1, or the cysteine mutants were treated with uptake buffer (white bars) or 10 mM MTSES (black bars) for 10 min at 37 °C. After the cells were washed, cell uptake of (A) 0.1 μM [<sup>3</sup>H]estrone-3-sulfate or (B) 1 μM [<sup>3</sup>H]estradiol-17β-glucuronide was measured at 37 °C for 30 s or for 2 min, respectively. Results were normalized for surface expression and are presented as percentage of each control. Each bar is the mean ± SD of three individual experiments. An asterisk (\*) indicates values significantly different from its control ( $p < 0.05$ ).

His antibody. If a free cysteine residue of the transporter was available, maleimide biotinylation would result in a band on the Western blot. As can be seen in Figure 5 (control), only mutant L545C reacts with maleimide-biotin, confirming that none of the cysteine residues present in wild-type OATP1B1 are accessible to maleimide and therefore suggesting that all extracellular cysteine residues form disulfide bonds or are otherwise inaccessible. However, after replacing the leucine residue at position 545 with a cysteine, this cysteine residue is accessible to maleimide-biotin and a band can be seen on the Western blot. Cells were also treated with maleimide-biotin after a preincubation with 10 mM MTSES (Figure 5, MTSES), a mixture of 10 mM MTSES and 1 mM estrone-3-sulfate (Figure 5, MTSES + E3S), or a mixture of 10 mM MTSES and 0.75 mM estradiol-17β-glucuronide (Figure 5, MTSES + E17βG). Maleimide biotinylation of L545C was completely prevented by preincubation with MTSES, indicating that L545C indeed reacted with MTSES. Simultaneous preincubation of MTSES with estrone-3-sulfate, fully restored maleimide

biotinylation of L545C to the control level, suggesting that estrone-3-sulfate protected MTSES labeling of L545C. However, protection of MTSES labeling was not observed with estradiol-17β-glucuronide, whose transport was actually stimulated in the presence of MTSES.

To test whether the observed effects were due to the negative charge introduced by MTSES or a steric effect of MTSES, we treated cells expressing wild-type OATP1B1 and certain mutants with the positively charged and membrane impermeable MTSET. The results are summarized in Figure 6 and demonstrate that estrone-3-sulfate uptake of mutant L545C was also strongly inhibited by MTSET (Figure 6A), indicating that MTSES and MTSET have more likely a steric effect than an effect due to the charge of the modifying reagent. Similarly, MTSET slightly inhibited estrone-3-sulfate uptake of G551C and V556C as did MTSES (Figure 6A). However, in contrast to MTSES, there was no inhibition of estrone-3-sulfate uptake by MTSET treatment of T553C. Furthermore, while MTSES treatment of S548C and H555C did not affect estrone-3-sulfate

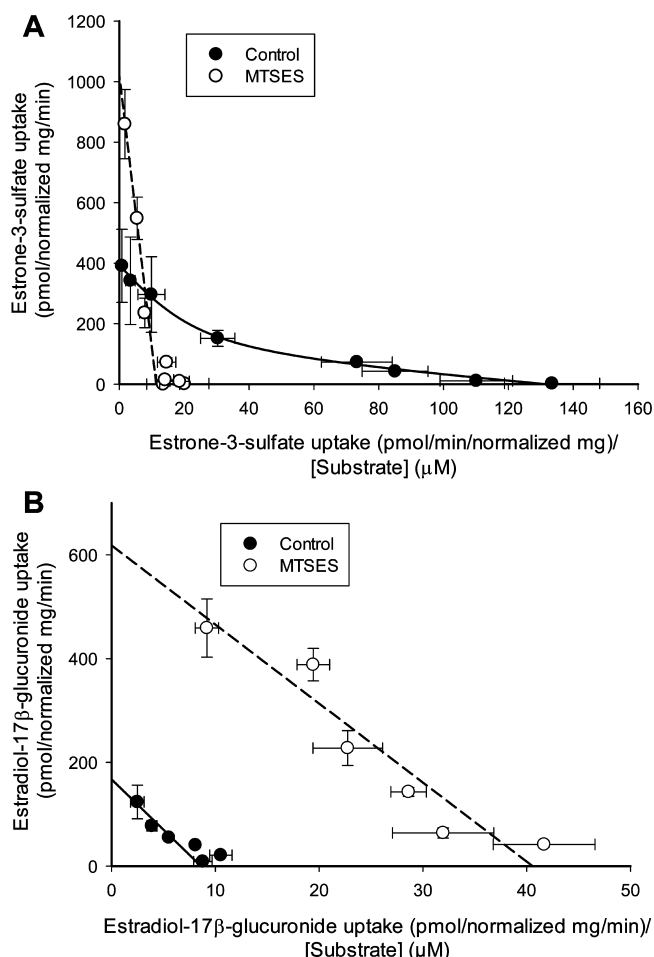


**Figure 4.** Eadie–Hofstee plots of kinetics for estrone-3-sulfate and estradiol-17β-glucuronide uptake by L545C in the presence and absence of MTSES. HEK293 cells transfected with empty vector or L545C were treated with uptake buffer (black circles) or 10 mM MTSES (white circles) for 10 min at 37 °C. After the cells were washed, uptake of (A) [<sup>3</sup>H]estrone-3-sulfate and (B) [<sup>3</sup>H]estradiol-17β-glucuronide was measured with increasing substrate concentrations (0.02–500 μM for estrone-3-sulfate and 1–50 μM for estradiol-17β-glucuronide) at 37 °C for 20 s (estrone-3-sulfate) or 1 min (estradiol-17β-glucuronide). Net uptake was calculated by subtracting the values obtained with empty vector transfected cells from L545C-expressing cells and normalized for surface expression. Each value is the mean ± SD of three individual experiments. Lines were drawn using the Enzyme kinetics function of SIGMAPLOT 12.

**Table 1. Kinetic Parameters of Estrone-3-sulfate (E3S) and Estradiol-17β-glucuronide (E17βG) Uptake by L545C in the Absence and Presence of MTSES<sup>a</sup>**

substrate	treatment	$K_m$ (μM)	$V_{max}$ (pmol/normalized mg/min)
E3S	control [BS1]	0.9 ± 0.6	95.9 ± 45.3
	[BS2]	15.6 ± 4.8	298 ± 42.2
	MTSES	89.7* ± 20.0	1018* ± 75.1
E17βG	control	19.4 ± 8.7	167 ± 33.7
	MTSES	15.2 ± 3.7	618* ± 64.0

<sup>a</sup>BS1: binding site 1; BS2: binding site 2. An asterisk (\*) indicates values significantly different from each control ( $p < 0.05$ ).

uptake and treatment of G552C resulted in a stimulation of uptake, treatment of all three mutants with MTSET resulted in

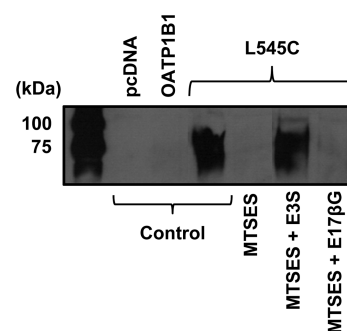


**Figure 5.** Effect of MTSES, estrone-3-sulfate, and estradiol-17β-glucuronide on maleimide labeling of L545C. Empty vector, OATP1B1, and L545C transfected HEK 293 cells were preincubated with uptake buffer (control), 10 mM MTSES (MTSES), a mixture of 10 mM MTSES and 1 mM estrone-3-sulfate (MTSES + E3S), or a mixture of 10 mM MTSES and 0.75 mM estradiol-17β-glucuronide (MTSES + E17βG) for 10 min at 37 °C to react and thus label the accessible cysteine residue with MTSES. After the cells were washed, they were treated with maleimide-PEG<sub>2</sub>-biotin for 1 h at 4 °C. Then, cell lysates were reacted with NeutrAvidin, and bound proteins were subjected to Western blot analysis with an anti-His antibody.

inhibition. For estradiol-17β-glucuronide, MTSET treatment had either no effect (N544C and V556C) or inhibited uptake (L545C, G552C, and H555C) but did not stimulate as MTSES (Figure 6B). Mutants G552C and H555C were affected in a similar way because both MTSES and MTSET inhibited estradiol-17β-glucuronide uptake.

The results presented so far strongly suggest that L545 might be part of the estrone-3-sulfate binding site/translocation pathway, and thus that leucine at position 545 is crucial for proper estrone-3-sulfate transport. Therefore, we replaced leucine at position 545 with random amino acids and compared the uptake of estrone-3-sulfate of these mutants with wild-type OATP1B1 (Figure 7). We used PROVEAN<sup>26</sup> and SNAP,<sup>27</sup> two algorithms available online that predict the effect amino acid replacements have on the biological function of proteins. Although both algorithms predicted all the tested replacements to be neutral, estrone-3-sulfate uptake was strongly reduced for all but the asparagine replacement, supporting the conclusion that L545 is important for OATP1B1-mediated estrone-3-sulfate transport.

Because it has been reported that OATP1B1 can transport valsartan,<sup>28</sup> we used valsartan as a model drug substrate and determined the uptake of valsartan by cysteine mutants from N544 to V556 because mutants in this range showed effects for estrone-3-sulfate and estradiol-17β-glucuronide transport. As can be seen from Figure 8A, all mutants were able to transport valsartan, even A549C which transported less than 20% of estrone-3-sulfate and estradiol-17β-glucuronide when compared to wild-type OATP1B1 showed a similar valsartan uptake as OATP1B1 (Figure 8A). We pretreated the mutants with MTSES or MTSET to test whether transport of this commonly used drug would be similarly affected by cysteine modifications and whether there would be charge effects. MTSES pretreatment reduced uptake of mutants L545C, A549C, G551C, G552C, and H555C (Figure 8B, black bars). Similarly, MTSET pretreatment did not stimulate valsartan uptake (Figure 8B, gray bars). In contrast to MTSES pretreatment, mutant H555C was not affected by MTSET pretreatment, suggesting that the effect of MTSES at this amino acid position is possibly a charge effect. All other mutants were

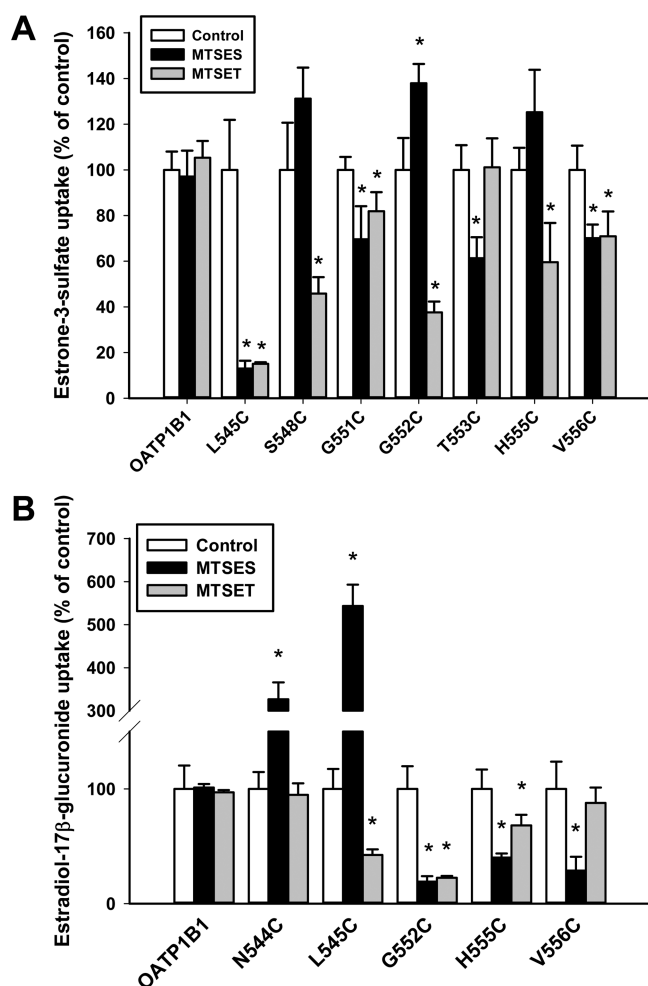


**Figure 6.** Comparison of the effect of MTSES and of MTSET on estrone-3-sulfate and estradiol-17 $\beta$ -glucuronide uptake by OATP1B1 and selected TM10 cysteine mutants. HEK293 cells transiently transfected with empty vector, OATP1B1, and its cysteine mutants were treated with uptake buffer (white bars), 10 mM MTSES (black bars), or 10 mM MTSET (gray bars) for 10 min at 37 °C. After the cells were washed, uptake of (A) 0.1  $\mu$ M [ $^3$ H]estrone-3-sulfate or (B) 1  $\mu$ M [ $^3$ H]estradiol-17 $\beta$ -glucuronide was measured at 37 °C for 30 s or for 2 min, respectively. Results were normalized for surface expression and are presented as the percentage of each control. Each bar is the mean  $\pm$  SD of three (MTSES and MTSET) or six (control) individual experiments. An asterisk (\*) indicates values significantly different from its control ( $p < 0.05$ ).

inhibited (L545C and A549C) or tended to be inhibited (G551C and G552C) by MTSET, suggesting that these effects were steric rather than charge-dependent. When comparing the amino acid residues that, when pretreated with MTSES, resulted in inhibition or stimulation of transport of the three tested substrates (Figure 9), it becomes clear that the different substrates need a similar but not identical set of residues within TM10 with which they interact.

## DISCUSSION

In this study, we used cysteine scanning mutagenesis of TM10 in OATP1B1 to determine accessibility and potential involvement of the mutated amino acid residues in the substrate binding site/translocation pathway. Our data indicate that estrone-3-sulfate, estradiol-17 $\beta$ -glucuronide, and valsartan

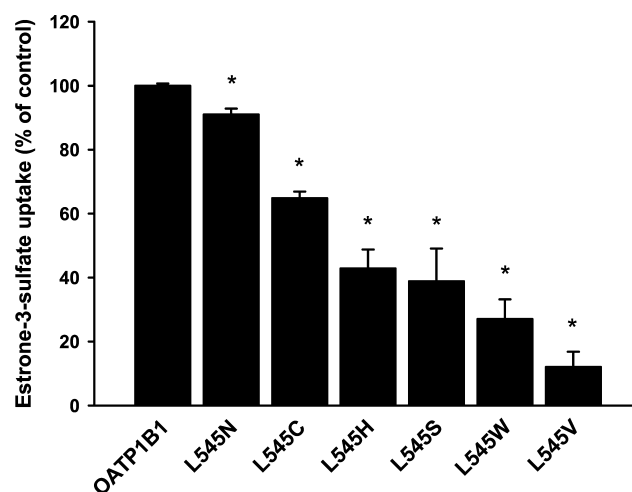


**Figure 7.** Effect of random mutagenesis of L545 on OATP1B1-mediated estrone-3-sulfate uptake. HEK293 cells were transiently transfected with empty vector, OATP1B1, or some randomly generated mutants. Uptake of 0.1  $\mu$ M [ $^3$ H]estrone-3-sulfate was measured for 1 min at 37 °C, and results for empty vector transfected cells were subtracted from OATP1B1 or mutant expressing cells. Results are given as means  $\pm$  SD of three individual experiments. An asterisk (\*) indicates values significantly different from OATP1B1 ( $p < 0.05$ ).

are transported by OATP1B1 using overlapping but not mutually exclusive binding sites/translocations pathways.

MTSES as well as MTSET preincubation of wild-type OATP1B1 did not affect transport of estrone-3-sulfate, estradiol-17 $\beta$ -glucuronide, or valsartan, indicating that similar to OATP2B1<sup>29</sup> all extracellular cysteine residues form disulfide bonds and cannot react with these cysteine reactive reagents or that reaction with existing cysteines does not affect the function. In addition, most of the 34 mutants were not affected by MTSES pretreatment, and the mutants that were affected are within the cytoplasmic half of the putative TM10.

Although transport of the three substrates was affected by MTSES labeling of very similar amino acid positions (Figure 9), there were clear differences. The most prominent difference was that labeling of L545C by MTSES inhibited estrone-3-sulfate and valsartan uptake but stimulated transport of estradiol-17 $\beta$ -glucuronide (Figures 3A,B and 8B). Because the compelling inhibition of estrone-3-sulfate and stimulation of estradiol-17 $\beta$ -glucuronide, we performed kinetics for these two substrates. For estrone-3-sulfate, kinetic analyses revealed that the mutant L545C exhibited biphasic kinetics (Figure 4A, Table 1) similar to the wild-type OATP1B1.<sup>20,24,25</sup> However, after labeling with MTSES, both the apparent  $K_m$  value and the  $V_{max}$  value increased, and the data could no longer be fitted to biphasic but only to monophasic kinetics. Thus, pretreatment with MTSES resulted in a transporter that when compared to wild-type OATP1B1 had a lower affinity and a higher capacity to transport estrone-3-sulfate. When we previously compared OATP1B1 with OATP1B3 with respect to estrone-3-sulfate transport, OATP1B3 was the transporter with the lower affinity and higher capacity.<sup>15</sup> Therefore, MTSES pretreatment of the OATP1B1 L545C mutant converts this transport protein into a functional OATP1B3, at least with respect to estrone-3-sulfate uptake. Whether the same is true for other substrates will have to be determined in future studies. The importance of L545 for estrone-3-sulfate uptake was already documented previously,<sup>20</sup>

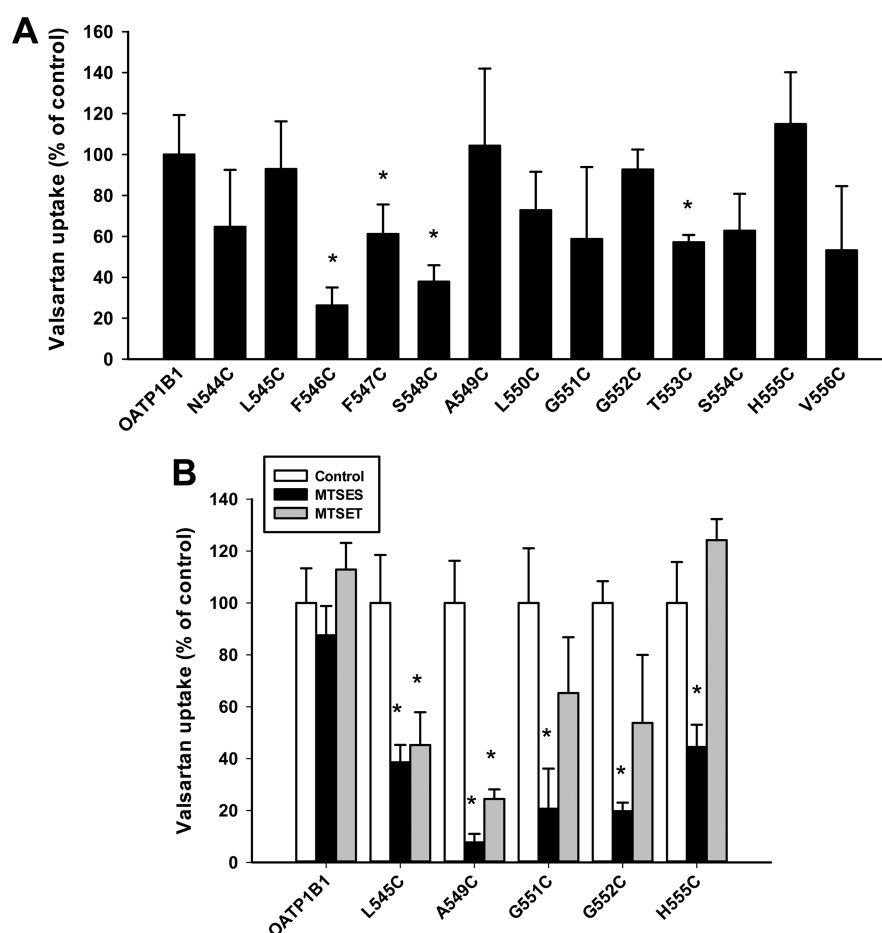


**Figure 8.** Effect of cysteine mutation and MTSES or MTSET treatment on valsartan uptake mediated by OATP1B1 and its TM10 cysteine mutants. HEK293 cells were transiently transfected with empty vector, OATP1B1, and its cysteine mutants. (A) Uptake of 1  $\mu$ M valsartan was measured for 8 min at 37  $^{\circ}$ C by LC/MS/MS, and results are given as percentage of uptake activity for OATP1B1. (B) Cells were treated with uptake buffer or 10 mM MTSES for 10 min at 37  $^{\circ}$ C. After the cells were washed, uptake of 1  $\mu$ M valsartan was measured for 8 min at 37  $^{\circ}$ C by LC/MS/MS. Results were normalized for surface expression and are presented as the percentage of each control. Each bar is the mean  $\pm$  SD of three individual experiments. An asterisk (\*) indicates values significantly different from its control ( $p < 0.05$ ).

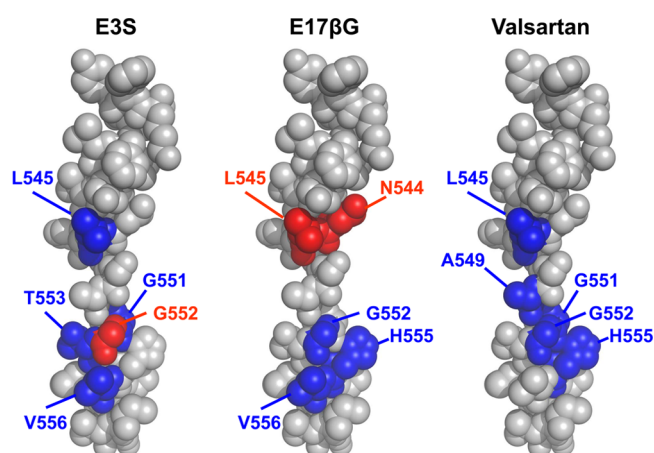


**Figure 9.** Graphical representation of residues 534–560 (top to bottom) in TM10 of OATP1B1. Residues where MTSES inhibited estrone-3-sulfate (E3S), estradiol-17 $\beta$ -glucuronide (E17 $\beta$ G), or valsartan are labeled blue; residues where MTSES stimulated substrate uptake are labeled red.

and more recent findings extended this for the OATP1B3 specific substrate cholecystokinin 8. When the three amino acids at positions 45, 545, and 615 in OATP1B1 were replaced

by their OATP1B3 counterparts, OATP1B1 was able to transport cholecystokinin 8,<sup>22</sup> further supporting the importance of L545 for OATP1B1 transport.

The suggestion that L545 might be part of the estrone-3-sulfate binding site/translocation pathway was confirmed by maleimide labeling experiments that demonstrated protection of MTSES labeling by estrone-3-sulfate but not by estradiol-17 $\beta$ -glucuronide (Figure 5) and by the fact that MTSES labeling changed the apparent affinity for estrone-3-sulfate transport, although it did not affect the apparent affinity for estradiol-17 $\beta$ -glucuronide uptake (Table 1).

Kinetic analysis performed for estradiol-17 $\beta$ -glucuronide uptake of L545C revealed that the apparent  $K_m$  value of 19.4  $\mu$ M (Table 1) was higher than the values (3.8–9.7  $\mu$ M) reported previously,<sup>24,30–33</sup> suggesting that the cysteine at this position might have an effect on estradiol-17 $\beta$ -glucuronide binding. However, there was no further effect of MTSES pretreatment on apparent affinity. Nevertheless, treatment with MTSES increased the maximal transport rate of estradiol-17 $\beta$ -glucuronide uptake by about 4-fold ( $V_{max}$  of 167 pmol/normalized mg/min in control versus  $V_{max}$  of 618 pmol/normalized mg/min in MTSES), suggesting that the stimulation of estradiol-17 $\beta$ -glucuronide uptake could be due to accelerated translocation of the substrate through OATP1B1



perhaps by facilitating interaction of the substrate with the protein in an optimal configuration due to the negative charge of MTSES. This hypothesis is supported by the finding that treatment with the cationic MTSET inhibited estradiol-17 $\beta$ -glucuronide uptake by about 60% (Figure 6B), indicating that indeed the negative charge of MTSES contributed to the marked stimulation of estradiol-17 $\beta$ -glucuronide uptake by LS45C and that the positive charge attached to the protein through MTSET hinders such an optimized configuration of estradiol-17 $\beta$ -glucuronide within the binding pocket of OATP1B1. An alternative explanation would be that the additional positive charge brought into the presumable binding pocket that already contains several important positively charged amino acids would increase the binding strength for negatively charged substrates and lead to an inhibition of transport via an increase in the apparent affinity as for example seen for mutations at position R580 for estradiol-17 $\beta$ -glucuronide, estrone-3-sulfate, and bromosulphophthalein uptake.<sup>21</sup> However, because the apparent affinity is not affected, LS45 does not seem to be close to the estradiol-17 $\beta$ -glucuronide binding site (translocation pathway). A similar but less pronounced stimulation/inhibition of the different substrates was observed with mutant G552C. While MTSES labeling stimulated estrone-3-sulfate uptake, it inhibited uptake of estradiol-17 $\beta$ -glucuronide and valsartan (Figures 3AB and 8B).

Mutant A549C which showed dramatically reduced estrone-3-sulfate and estradiol-17 $\beta$ -glucuronide transport (Figure 2) had normal transport of valsartan (Figure 8). Pretreatment with MTSES as well as with MTSET resulted in a very strong inhibition of valsartan uptake. Besides amino acids affecting more than one substrate, we also identified residues that only affected transport of one of the three substrates: labeling of N544C with MTSES stimulated estradiol-17 $\beta$ -glucuronide uptake but did not affect transport of estrone-3-sulfate (Figure 3) or valsartan (data not shown) uptake. Taken together, these results demonstrate clearly that a set of common but not identical amino acids are involved in the substrate binding sites/translocation pathways for the different OATP1B1 substrates.

In conclusion, our results demonstrate that several amino acids in the cytoplasmic half of TM10 of OATP1B1 are part of the substrate binding site/translocation pathway. While none of the three tested substrates is handled in the exact same way, this study identified five amino acids that are particularly important for the transport of all the three substrates. Among these, the leucine at position 545 seems to be part of the estrone-3-sulfate binding site/translocation pathway. Thus, the present study provides novel insight toward a better understanding of the multispecificity of OATP1B1 at the molecular level.

## AUTHOR INFORMATION

### Corresponding Author

\*Address: Department of Pharmacology, Toxicology and Therapeutics, The University of Kansas Medical Center, 3901 Rainbow Blvd., Kansas City, KS 66160. Phone: 913-588-0028. Fax: 913-588-7501. E-mail: bhagenbuch@kumc.edu.

### Funding

This work was supported by National Institute of Health Grants RR021940, GM077336, GM103549, and ES07079.

### Notes

The authors declare no competing financial interest.

## ACKNOWLEDGMENTS

We thank Colleen Flynn and Greg Reed for their help with valsartan determination by LC/MS/MS.

## ABBREVIATIONS

TM10, transmembrane domain 10; MTSES, sodium (2-sulfonatoethyl)methanethiosulfonate; MTSET, [2-(trimethylammonium)ethyl]methanethiosulfonate bromide; OATP, organic anion transporting polypeptide

## REFERENCES

- (1) Hagenbuch, B., and Stieger, B. (2013) The SLCO (former SLC21) superfamily of transporters. *Mol. Aspects Med.* 34, 396–412.
- (2) König, J. (2011) Uptake transporters of the human OATP family: Molecular characteristics, substrates, their role in drug-drug interactions, and functional consequences of polymorphisms. *Handb. Exp. Pharmacol.* 201, 1–28.
- (3) Hagenbuch, B., and Gui, C. (2008) Xenobiotic transporters of the human organic anion transporting polypeptides (OATP) family. *Xenobiotica* 38, 778–801.
- (4) König, J., Cui, Y., Nies, A. T., and Keppler, D. (2000) A novel human organic anion transporting polypeptide localized to the basolateral hepatocyte membrane. *Am. J. Physiol.* 278, G156–G164.
- (5) Roth, M., Obaidat, A., and Hagenbuch, B. (2012) OATPs, OATs and OCTs: the organic anion and cation transporters of the SLCO and SLC22A gene superfamilies. *Br. J. Pharmacol.* 165, 1260–1287.
- (6) Park, J. W., Siekmeier, R., Lattke, P., Merz, M., Mix, C., Schuler, S., and Jaross, W. (2001) Pharmacokinetics and pharmacodynamics of fluvastatin in heart transplant recipients taking cyclosporine A. *J. Cardiovasc. Pharmacol. Ther.* 6, 351–361.
- (7) Regazzi, M. B., Iacona, I., Campana, C., Raddato, V., Lesi, C., Perani, G., Gavazzi, A., and Vigano, M. (1993) Altered disposition of pravastatin following concomitant drug therapy with cyclosporin A in transplant recipients. *Transplant. Proc.* 25, 2732–2734.
- (8) Simonson, S. G., Raza, A., Martin, P. D., Mitchell, P. D., Jarcho, J. A., Brown, C. D., Windass, A. S., and Schneek, D. W. (2004) Rosuvastatin pharmacokinetics in heart transplant recipients administered an antirejection regimen including cyclosporine. *Clin. Pharmacol. Ther.* 76, 167–177.
- (9) Link, E., Parish, S., Armitage, J., Bowman, L., Heath, S., Matsuda, F., Gut, I., Lathrop, M., and Collins, R. (2008) SLCO1B1 variants and statin-induced myopathy - a genomewide study. *N. Engl. J. Med.* 359, 789–799.
- (10) Chang, C., Ekins, S., Bahadduri, P., and Swaan, P. W. (2006) Pharmacophore-based discovery of ligands for drug transporters. *Adv. Drug Delivery Rev.* 58, 1431–1450.
- (11) Karlgren, M., Ahlin, G., Bergstrom, C. A., Svensson, R., Palm, J., and Artursson, P. (2012) In vitro and in silico strategies to identify OATP1B1 inhibitors and predict clinical drug-drug interactions. *Pharm. Res.* 29, 411–426.
- (12) Chang, C., Pang, K. S., Swaan, P. W., and Ekins, S. (2005) Comparative pharmacophore modeling of organic anion transporting polypeptides: A meta-analysis of rat OATP1A1 and human OATP1B1. *J. Pharmacol. Exp. Ther.* 314, 533–541.
- (13) Gui, C., Wahlgren, B., Lushington, G. H., and Hagenbuch, B. (2009) Identification, K<sub>i</sub> determination and CoMFA analysis of nuclear receptor ligands as competitive inhibitors of OATP1B1-mediated estradiol-17 $\beta$ -glucuronide transport. *Pharmacol. Res.* 60, 50–56.
- (14) Meier-Abt, F., Mokrab, Y., and Mizuguchi, K. (2005) Organic anion transporting polypeptides of the OATP/SLCO superfamily: identification of new members in nonmammalian species, comparative modeling and a potential transport mode. *J. Membr. Biol.* 208, 213–227.
- (15) Gui, C., and Hagenbuch, B. (2008) Amino acid residues in transmembrane domain 10 of organic anion transporting polypeptide

1B3 are critical for cholecystokinin octapeptide transport. *Biochemistry* 47, 9090–9097.

(16) Mandery, K., Sticht, H., Bujok, K., Schmidt, I., Fahrmayr, C., Balk, B., Fromm, M. F., and Glaeser, H. (2011) Functional and structural relevance of conserved positively charged lysine residues in organic anion transporting polypeptide 1B3. *Mol. Pharmacol.* 80, 400–406.

(17) Li, N., Hong, W., Huang, H., Lu, H., Lin, G., and Hong, M. (2012) Identification of amino acids essential for estrone-3-sulfate transport within transmembrane domain 2 of organic anion transporting polypeptide 1B1. *PLoS One* 7, e36647.

(18) Huang, J., Li, N., Hong, W., Zhan, K., Yu, X., Huang, H., and Hong, M. (2013) Conserved tryptophan residues within putative transmembrane domain 6 affect transport function of organic anion transporting polypeptide 1B1. *Mol. Pharmacol.* 84, 521–527.

(19) Miyagawa, M., Maeda, K., Aoyama, A., and Sugiyama, Y. (2009) The eighth and ninth transmembrane domains in organic anion transporting polypeptide 1B1 affect the transport kinetics of estrone-3-sulfate and estradiol-17 $\beta$ -D-glucuronide. *J. Pharmacol. Exp. Ther.* 329, 551–557.

(20) Gui, C., and Hagenbuch, B. (2009) Role of transmembrane domain 10 for the function of organic anion transporting polypeptide 1B1. *Protein Sci.* 18, 2298–2306.

(21) Weaver, Y. M., and Hagenbuch, B. (2010) Several conserved positively charged amino acids in OATP1B1 are involved in binding or translocation of different substrates. *J. Membr. Biol.* 236, 279–290.

(22) DeGorter, M. K., Ho, R. H., Leake, B. F., Tirona, R. G., and Kim, R. B. (2012) Interaction of three regiospecific amino acid residues is required for OATP1B1 gain of OATP1B3 substrate specificity. *Mol. Pharm.* 9, 986–995.

(23) Ho, R. H., Leake, B. F., Roberts, R. L., Lee, W., and Kim, R. B. (2004) Ethnicity-dependent polymorphism in Na<sup>+</sup>-taurocholate cotransporting polypeptide (SLC10A1) reveals a domain critical for bile acid substrate recognition. *J. Biol. Chem.* 279, 7213–7222.

(24) Tamai, I., Nozawa, T., Koshida, M., Nezu, J., Sai, Y., and Tsuji, A. (2001) Functional characterization of human organic anion transporting polypeptide B (OATP-B) in comparison with liver-specific OATP-C. *Pharm. Res.* 18, 1262–1269.

(25) Noe, J., Portmann, R., Brun, M. E., and Funk, C. (2007) Substrate-dependent drug-drug interactions between gemfibrozil, fluvastatin and other organic anion-transporting peptide (OATP) substrates on OATP1B1, OATP2B1, and OATP1B3. *Drug Metab. Dispos.* 35, 1308–1314.

(26) Choi, Y., Sims, G. E., Murphy, S., Miller, J. R., and Chan, A. P. (2012) Predicting the functional effect of amino acid substitutions and indels. *PLoS One* 7, e46688.

(27) Bromberg, Y., and Rost, B. (2007) SNAP: predict effect of non-synonymous polymorphisms on function. *Nucleic Acids Res.* 35, 3823–3835.

(28) Yamashiro, W., Maeda, K., Hirouchi, M., Adachi, Y., Hu, Z., and Sugiyama, Y. (2006) Involvement of transporters in the hepatic uptake and biliary excretion of valsartan, a selective antagonist of the angiotensin II AT1-receptor, in humans. *Drug Metab. Dispos.* 34, 1247–1254.

(29) Hänggi, E., Grundschober, A. F., Leuthold, S., Meier, P. J., and St-Pierre, M. V. (2006) Functional analysis of the extracellular cysteine residues in the human organic anion transporting polypeptide, OATP2B1. *Mol. Pharmacol.* 70, 806–817.

(30) Gui, C., Miao, Y., Thompson, L., Wahlgren, B., Mock, M., Stieger, B., and Hagenbuch, B. (2008) Effect of pregnane X receptor ligands on transport mediated by human OATP1B1 and OATP1B3. *Eur. J. Pharmacol.* 584, 57–65.

(31) Nakai, D., Nakagomi, R., Furuta, Y., Tokui, T., Abe, T., Ikeda, T., and Nishimura, K. (2001) Human liver-specific organic anion transporter, LST-1, mediates uptake of pravastatin by human hepatocytes. *J. Pharmacol. Exp. Ther.* 297, 861–867.

(32) König, J., Cui, Y., Nies, A. T., and Keppler, D. (2000) Localization and genomic organization of a new hepatocellular organic anion transporting polypeptide. *J. Biol. Chem.* 275, 23161–23168.

(33) Hirano, M., Maeda, K., Shitara, Y., and Sugiyama, Y. (2004) Contribution of OATP2 (OATP1B1) and OATP8 (OATP1B3) to the hepatic uptake of pitavastatin in humans. *J. Pharmacol. Exp. Ther.* 311, 139–146.